

# 1

## Compression of Slender Struts

### 1.1 Introduction

The stress  $\sigma$  within a long slender strut of uniform cross-section is affected by the magnitude of the load applied  $P$  and its length  $L$ . It will be shown that the weight of the strut is a minimum when the stress is a maximum. It is therefore necessary to investigate how  $\sigma$  varies with both  $P$  and  $L$  and the shape of the cross-section, each being under the control of the designer. The general approach is to seek an objective function in which the strut's weight  $W$  is expressed as the product of the strut's volume and density  $\rho$ . This gives

$$W = \rho AL = \rho \left( \frac{P}{\sigma} \right) L = \frac{PL}{\sigma/\rho} \quad (1.1)$$

where the elastic stress  $\sigma$  in the strut prior to its buckling is equated to the axial load per unit area, i.e.  $\sigma = P/A$ , and  $L$  is the 'pinned' strut length. Hence, to minimise  $W$  it follows from equation (1.1) that  $\sigma/\rho$ , the equivalent objective function, is to be maximised. The following failure criteria provide the various limiting stress measures upon which the strut's minimum weight is to be based.

### 1.2 Failure Criteria

The failure criteria for a strut would need to be expressed in terms of the section's shape, whether this be solid, hollow, thin-walled, tubular, etc.

#### 1.2.1 Flexural Buckling

Euler's theory [1] expresses the critical elastic buckling load  $P_c$  for a pinned-end strut as

$$P_c = \frac{\pi^2 EI}{L^2} \quad (1.2a)$$

where  $I = Ak^2$  is the least second moment of area, which depends upon the radius of gyration of the section. Hence, the critical flexural buckling stress  $\sigma_F$  may be expressed as

$$\sigma_F = \frac{\pi^2 E}{(L/k)^2} \quad (1.2b)$$

In shorter, stockier struts, where buckling is elastic-plastic, the tangent modulus  $E_T$  may replace the elastic modulus  $E$  in equations (1.2a,b).

### 1.2.2 Local Buckling

A local buckling failure refers specifically to struts with thin walls in their cross-sections. Typically, this mode of failure appears as an indentation of diamond shape upon the surface or in a bowing of the section walls [2]. Local buckling does not arise in struts with solid sections. For buckling of the flat plates (i.e. the walls) within thin-walled tubular sections, the local buckling stress takes the form [3]

$$\sigma_L = K_L E_T \left( \frac{t}{d} \right) \quad (1.3)$$

where  $K_L$  is a buckling coefficient that depends upon the plates aspect ratio and the support provided to its edges (see equation (D.1a,b) in Appendix D).

### 1.2.3 Working Stress

In the absence of buckling, the axial, compressive, working stress  $\sigma_W$  is found simply by dividing the applied load  $P$  by the section area  $A$ :

$$\sigma_W = \frac{P}{A} \quad (1.4)$$

### 1.2.4 Limiting Stress

The stress in equations (1.2b), (1.3) and (1.4) would normally be limited to the yield stress where buckling is elastic. In the case of plastic buckling the limiting stress is raised to correspond to a given offset (plastic) strain, i.e. the 0.1% proof stress. Let  $\sigma_y$  be the limiting yield or proof stress of the strut material appropriate to its buckling behaviour. Then, its relation to the applied stress ( $\sigma_F$ ,  $\sigma_L$  and  $\sigma_W$  above) from those sources in equations (1.2b)–(1.4), is simply

$$\sigma \leq \sigma_y \quad (1.5)$$

### 1.2.5 Objective Function

An optimum section size is found by equating (1.2b), (1.3) (where appropriate) and (1.4), where they all have been limited by equation (1.5). Finally, all appropriate failure criteria in § 1.2.1–1.2.4 are combined within the objective function to minimise the weight. We



**Figure 1.1** Standard, solid strut cross-sections

shall demonstrate this design procedure, firstly, with the more common solid cross-sections in Figure 1.1.

### 1.3 Solid Cross-Sections

The four solid cross-section shown in Figure 1.1 are the most likely contenders for strut cross-sections as these are available in long bars of extruded stock.

#### 1.3.1 Circular Section, Diameter $d$ (see Figure 1.1a)

With  $I = \pi d^4 / 64$ , then  $k^2 = d^2 / 16$  and the buckling failure criterion (1.2a), becomes

$$\sigma_F = \frac{\pi^2 E d^2}{16 L^2} \tag{1.6}$$

When equation (1.6) is combined with the axial stress formula (1.4) with  $A = \pi d^2 / 4$ , so that  $\sigma_F = \sigma_W$ , this gives the optimum diameter:

$$d_{\text{opt}} = \frac{(64P)^{1/4} L^{1/2}}{\pi^{3/4} E^{1/4}} = 1.199 \left( \frac{PL^2}{E} \right)^{1/4} \tag{1.7a}$$

It will be seen that all solid sections will conform to an equation of similar form for an optimum section dimension (here the diameter) as:

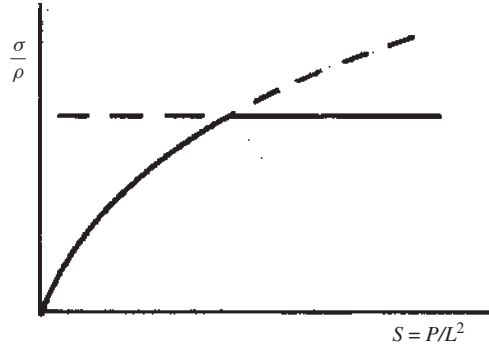
$$d_{\text{opt}} = C \left( \frac{PL^2}{E} \right)^{1/4} \tag{1.7b}$$

where  $C$  is a *shape coefficient*. Substituting equation (1.7a) into equation (1.6) and dividing by  $\rho$  leads to the equivalent objective function for a solid, circular-section strut:

$$\left( \frac{\sigma}{\rho} \right)_{\text{opt}} = 0.886 \left( \frac{E^{1/2}}{\rho} \right) \left( \frac{P}{L^2} \right)^{1/2} \tag{1.8a}$$

Here, a *shape efficiency factor*  $F = 0.886$  appears. The *material efficiency factor* is  $M = \sqrt{E/\rho}$  and the *structural index*  $S = P/L^2$  is raised to the fractional power  $1/2$ . Hence, we may write the quantity to be maximised, the *objective function*  $R$ , more generally as

$$R = \left( \frac{\sigma}{\rho} \right)_{\text{opt}} = F \times M \times S^n \tag{1.8b}$$



**Figure 1.2** Objective function plot from equation (1.8a) showing limiting stress cut-off

where, for a circular cross-section,  $n = 1/2$ . If we wish to employ a tangent modulus  $E_T$  this will reduce  $M$  by the ratio  $\sqrt{(E_T/E)}$ . We can derive from equation (1.8a) the plot given in Figure 1.2 with limiting stress cut-offs at an appropriate yield, proof or ultimate stress level.

### 1.3.2 Solid Square Bar $a \times a$ (see Figure 1.1b)

With  $I = a^4/12$  and  $A = a^2$ , then  $k^2 = a^2/12$  and the buckling failure criterion, equation (1.2b), becomes

$$\sigma_F = \frac{\pi^2 E a^2}{12 L^2} \quad (1.9)$$

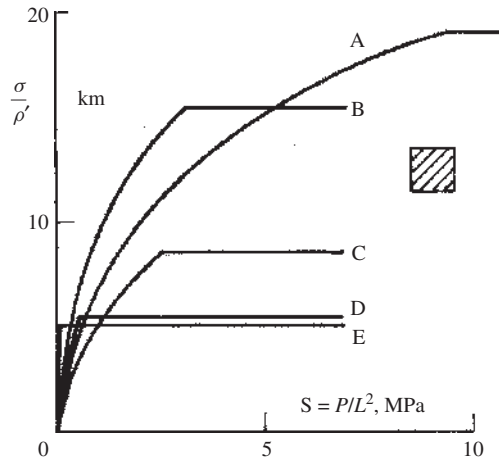
Equate (1.9) to the axial stress formula (1.4), i.e.  $\sigma_W = \sigma_F$ , and on setting  $A = a^2$ , this gives the square side length as

$$a_{\text{opt}} = \frac{(12P)^{1/4} L^{1/2}}{\pi^{1/2} E^{1/4}} = 1.050 \left( \frac{PL^2}{E} \right)^{1/4} \quad (1.10)$$

Substituting equation (1.10) into equation (1.9) and dividing by  $\rho$  leads to the objective function required:

$$\left( \frac{\sigma}{\rho} \right)_{\text{opt}} = 0.907 \left( \frac{E^{1/2}}{\rho} \right) \left( \frac{P}{L^2} \right)^{1/2} \quad (1.11)$$

Equation (1.11) is similar in form to the circular section's objective function, equation (1.8a). Note here that the greater value of the shape efficiency factor  $F = 0.907$  indicates that more of the material in the square section is fully stressed. Figure 1.3 presents equation (1.11) graphically for four materials whose properties and relevant ratios appear in Table 1.1 (see also Appendix A). The figure shows working stress ranges cut off by the limiting stress. The latter is taken to be the 0.1% proof stress for the metallic materials and the ultimate stress for Douglas fir and the glass fibre-reinforced composite (GFRC).



**Figure 1.3** Objective function versus structural index for struts with solid square sections (key: A, Ti alloy; B, Al alloy; C, steel; D, GFRC; E, Douglas fir (see Table 1.1))


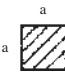


Within the range of the index  $S = P/L^2$  shown, the aluminium alloy (L65) appears to optimise the stress most efficiently at a given  $S$ . Notably, in extending the range of  $S$  threefold, titanium alloy (DTD 5053) allows higher objective functions to be reached. The high grade bolt steel (S96) is a poor performer on a weight/strength basis. GFRC lies between the aluminium and titanium alloys but is cut off at a much lower value,  $\sigma_{ult}/\rho = 5.7 \text{ km}$ . Douglas fir has a similar cut-off at  $5.1 \text{ km}$  and, within a very restricted range of structural indices ( $P/L^2 < 0.2$ ), provides the greatest objective function of all the materials considered within this figure. In this case both  $E$  and  $\sigma_{ult}$  are properties of fir taken parallel to the grain.

A similar analysis may be applied to a strut of any solid cross-section. Table 1.2 summarises the results obtained here for the circular and square sections together with those that apply to semi-circular and equilateral triangular sections (see Figure 1.1c,d). The comparison between the four sections may be made simply through the shape coefficient  $C$  and the shape factor  $F$ , appearing in equations (1.7b) and (1.8b). Of these four sections an equilateral triangle appears to bear the greatest stress. The implication of this is that when  $(\sigma/\rho)_{opt}$  is to be maximised, in order to minimise the strut’s weight, the triangular

**Table 1.1** Properties of common structural materials

Material\Property → ↓ Unit →	$E$ GPa	$\rho$ kg/m <sup>3</sup>	$E^{1/2}/\rho$ m <sup>2</sup> /N <sup>1/2</sup>	$E^{2/3}/\rho$ (m <sup>5</sup> /N) <sup>1/3</sup>	$E^{3/5}/\rho$ (m <sup>9</sup> /N <sup>2</sup> ) <sup>1/5</sup>
A Ti alloy (DTD 5053)	118	4540	7.22	494.6	9.2
B Al alloy (L65)	75	2790	9.83	634.6	119.8
C Steel (S96)	207	7800	5.79	441.7	78
D GFRC	20	1800	8	41.73	85.84
E Douglas fir	11	497	21.51	1014.47	217.18

**Table 1.2** Shape coefficients for slender struts of solid section

Cross-section				
$C$	1.199	1.050	1.960	1.539
$F$	0.886	0.907	0.663	0.975

section strut would provide the lowest weight for supporting a predetermined compressive load in a given material.

## 1.4 Thin-Walled, Tubular Sections

The objective function is again  $R = \sigma/\rho$ , but two cross-section variables arise in tubular sections: a mean section dimension  $d$  and the wall thickness  $t$  (see Figure 1.4a). Appendix D shows that failure criteria must now include local buckling in addition to flexural buckling. In deriving the objective function  $R$ , the usual procedure is to establish the failure criteria first. Then, by ensuring that the critical stresses by these criteria are attained simultaneously, the geometry of the tubular section is optimised, from which the usual form for  $R$  will follow.

### 1.4.1 Thin-Walled Circular Tube

Local, inelastic buckling in thin-walled circular tubes (Figure 1.4a) of moderate length under compression has been reported in [4]. Mostly, buckling appeared in the two-lobe failure mode (Figure 1.4b), even though four lobes are generally assumed for an elastic failure [2].

#### (i) Flexural Buckling

With  $I = \pi d^3 t/8$  and  $A \approx \pi dt$ , then  $k^2 = I/A \approx d^2/8$ . Hence the buckling stress in equation (1.2b) becomes

$$\sigma_F = \frac{\pi^2 E_T d^2}{8L^2} \quad (1.12)$$

#### (ii) Limiting Stress

The working, compressive stress  $\sigma_W$  in the strut is given as

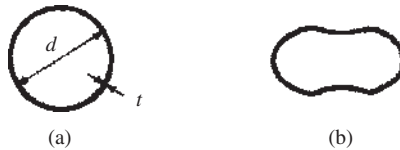
$$\sigma_W = \frac{P}{A} = \frac{P}{\pi dt} \quad (1.13)$$

which is limited to  $\sigma_y$ , i.e.  $\sigma_W \leq \sigma_y$ . (Here we take:  $\sigma_W = \sigma_y$ )

#### (iii) Local Buckling

A collapse of the wall surface occurs (see Figure 1.4b) when local depressions appear under an axial stress:

$$\sigma_L = K_L E_T \left( \frac{t}{d} \right) \quad (1.14)$$



**Figure 1.4** Circular tube section showing local wall buckling

The theoretical value of the buckling coefficient is  $K_L = 1.212$  but here the value  $K_L = 0.4$  is used as it has been found to match experimental data more closely [1].

*(iv) Optimisation*

A strut with optimum geometry is found by combining equations (1.12)–(1.14), so that the stresses by the three criteria are made equal,  $\sigma_F = \sigma_W = \sigma_L$ , which gives

$$\frac{\pi^2 E_T d^2}{8L^2} = \frac{P}{\pi dt} = 0.40 E_T \left(\frac{t}{d}\right) \tag{1.15}$$

Equation (1.15) allows optimum dimensions  $d$  and  $t$  to be found as

$$t_{\text{opt}} = \left(\frac{P}{\pi K_L E_T}\right)^{1/2} = 0.892 \left(\frac{P}{E_T}\right)^{1/2} \tag{1.16a}$$

$$d_{\text{opt}} = \left(\frac{8\sqrt{K_L}}{\sqrt{\pi^5}}\right)^{1/3} \left(\frac{PL^4}{E_T}\right)^{1/6} = 0.661 \left(\frac{PL^4}{E_T}\right)^{1/6} \tag{1.16b}$$

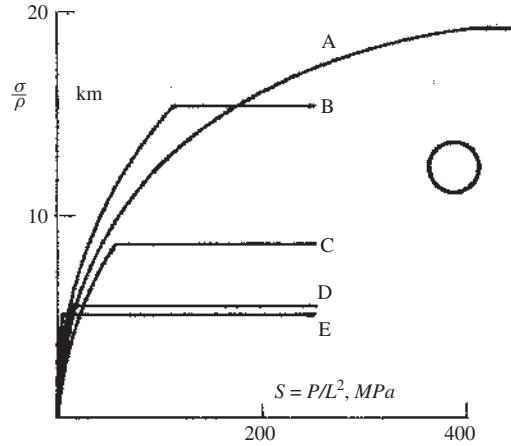
The optimum stress follows from substituting  $d_{\text{opt}}$  and  $t_{\text{opt}}$  into any of the three expressions in equation (1.15). Dividing by  $\rho$  gives the objective function

$$\left(\frac{\sigma}{\rho}\right)_{\text{opt}} = 0.540 \left(\frac{E_T^{2/3}}{\rho}\right) \left(\frac{P}{L^2}\right)^{1/3} \tag{1.17}$$

As the exponent of  $E_T$ , within the material factor  $M$ , differs from that of a solid circular section (see equation (1.8a)) a comparison between the contribution to  $R$  from the separate factors  $F$ ,  $M$  and  $S$  for the two sections would be inappropriate. However, the result of the product between  $F$ ,  $M$  and  $S$ , which gives  $R$ , provides the basis for the required weight to strength comparison. Figure 1.5 presents equation (1.17) graphically for four materials whose properties and relevant ratios appear in Table 1.1. Again, the aluminium alloy (L65) is the most efficient when the structural index  $S < 100$ , but beyond this the titanium alloy (DTD 5053) takes over, allowing  $S$  to reach 400 at its greatest limiting stress level.

*1.4.2 Thin-Walled Square Tube*

The uniform square tube (Figure 1.6a) has a mean side length  $a$  and wall thickness  $t$ . Local buckling (Figure 1.6b) appears in a bowing of the flat plates that comprise the walls.



**Figure 1.5** Objective function versus  $S$  for struts with thin-walled, circular tube sections (key: A, Ti alloy; B, Al alloy; C, steel; D, GFRC; E, Douglas fir (see Table 1.1))

As this form distortion of the section occurs without translation or rotation it is said to be local, i.e. it may exist together with the usual flexural buckling behaviour of a strut [2].

(i) *Flexural Buckling*

With  $I = 2a^3t/3$  and  $A \approx 4at$ , then  $k^2 = I/A \approx a^2/6$ . Hence, the buckling stress in equation (1.2b) becomes

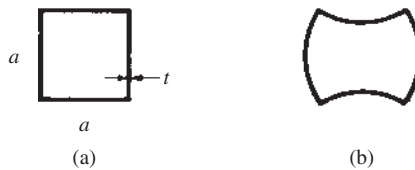
$$\sigma_F = \frac{\pi^2 E_T a^2}{6L^2} \tag{1.18}$$

(ii) *Limiting Stress*

The working, compressive stress in the strut is given as

$$\sigma_W = \frac{P}{A} = \frac{P}{4at} \tag{1.19}$$

where  $\sigma_W \leq \sigma_y$ , for a proof stress  $\sigma_y$  defined by an offset strain (typically 0.1% or 0.2%). Here the gradient to the stress–strain curve, corresponding to the stress level  $\sigma_y$ , is used to define the tangent modulus  $E_T$  in equation (1.18).



**Figure 1.6** Square tube section showing local wall buckling

*(iii) Local Buckling*

When each wall is taken as a long flat plate with simply supported edges (see Figure 1.6b), a lateral collapse occurs under an axial stress:

$$\sigma_L = K_L E_T \left( \frac{t}{a} \right)^2 \quad (1.20)$$

where the buckling coefficient  $K_L = 3.62$  for  $\nu = 0.3$  [3] (see Appendix D).

*(iv) Optimisation*

An optimum geometry is found by combining equations (1.18)–(1.20) so that the stresses by the three criteria (i), (ii) and (iii) above are made equal,  $\sigma_F = \sigma_W = \sigma_L$ , which gives

$$\frac{\pi^2 E_T a^2}{6L^2} = \frac{P}{4at} = 3.62 E_T \left( \frac{t}{a} \right)^2 \quad (1.21)$$

Equation (1.21) allows the optimum dimensions  $a$  and  $t$  to be written as

$$\begin{aligned} a_{\text{opt}} &= 0.743 \left( \frac{PL^3}{E_T} \right)^{1/5} \\ t_{\text{opt}} &= 0.371 \left( \frac{P^2L}{E_T^2} \right)^{1/5} \end{aligned} \quad (1.22a,b)$$

The optimum stress follows from substituting  $a_{\text{opt}}$  and  $t_{\text{opt}}$  into any of the three parts within equation (1.21). Dividing by  $\rho$  gives the required objective function:

$$\left( \frac{\sigma}{\rho} \right)_{\text{opt}} = 0.907 \left( \frac{E_T^{3/5}}{\rho} \right) \left( \frac{P}{L^2} \right)^{2/5} \quad (1.23)$$

Again, the material factor  $M$  differs from that of solid section, equation (1.11). Hence, a comparison between the separate contributions of the factors  $F$ ,  $M$  and  $S$  to  $R = (\sigma/\rho)_{\text{opt}}$  for the two sections cannot be made. However, the result of their products which define  $R$  in equation (1.23) provides the basis for the required weight to strength comparison (see Table 1.3).

*1.4.3 Thin-Walled Hexagonal Tube*

Following the analyses of the circular and square tubes, we may consider closed tubes with any number of sides. Similar analyses [5] to those given here reveal that regular polygons all have identical material efficiency factors and structural indices to that for the square tube. We give one example of a thin-walled, regular hexagon in Figure 1.7a.

**Table 1.3** Shape efficiency factors and buckling coefficients for thin-walled, tubular polygon strut sections

No of sides	$F$	$K_L$
3	0.789	4.31
4	0.907	3.62
5	1.031	3.87
6	1.112	3.62
7	1.203	3.76
8	1.268	3.62
9	1.340	3.69
10	1.396	3.62

(i) *Flexural Buckling*

The second moment of area about axis  $x$  has contributions from the two vertical sides and the four sloping sides (Figure 1.7b) as follows:

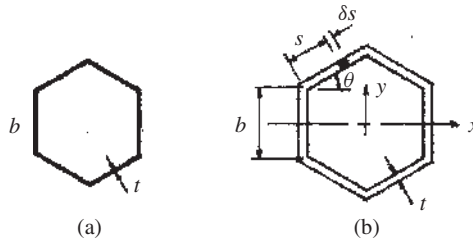
$$I_x = 2 \frac{tb^3}{12} + 4 \int_0^b \left( \frac{b}{2} + s \sin \theta \right)^2 t ds = \frac{5tb^3}{2} \tag{1.24a}$$

The second moment of area about axis  $y$  has contributions from the same two vertical sides and four sloping sides but in a different disposition:

$$I_y = 2 \left[ \frac{bt^3}{12} + bt(b \sin \theta) \right] + 4 \int_0^b (s \sin \theta)^2 t ds \tag{1.24b}$$

$$= \frac{bt^3}{6} + \frac{5tb^3}{2} \approx \frac{5tb^3}{2}$$

For practical purposes the two second moments may be assumed equal. Hence, buckling will occur about each axis simultaneously under a critical compressive load. With  $I = 5tb^3/2$  and  $A \approx 6bt$ , then  $k^2 = I/A = 5b^2/12$ . Hence the critical buckling stress in



**Figure 1.7** Hexagonal tube section showing the  $I_x$  calculation for a sloping wall

equation (1.2b) becomes

$$\sigma_F = \frac{5\pi^2 E_T b^2}{12L^2} \quad (1.25)$$

(ii) *Limiting Stress*

The working, compressive stress in the strut is given as

$$\sigma_W = \frac{P}{A} = \frac{P}{6bt} \quad (1.26)$$

where  $\sigma_W \leq \sigma_y$ , for a proof stress  $\sigma_y$  defined by an offset strain (typically 0.1% or 0.2%). The gradient to the stress–strain curve, corresponding to  $\sigma_y$ , defines the tangent modulus  $E_T$  in equation (1.25).

(iii) *Local Buckling*

When each wall surface is modelled as a long flat plate with simply supported corners, a critical, lateral bowing occurs in the manner of Figure 1.6b, under an axial stress:

$$\sigma_L = K_L E_T \left(\frac{t}{b}\right)^2 \quad (1.27)$$

where  $K_L = 3.62$  applies consistently to polygons with even numbers of sides (see Table 1.3).

(iv) *Optimisation*

*Method 1*

An optimum geometry is found by the usual method of combining (i), (ii) and (iii) above so that the stresses by the three criteria are made equal,  $\sigma_F = \sigma_W = \sigma_L$ , between equations (1.25)–(1.27), which gives

$$\frac{5\pi^2 E_T b^2}{12L^2} = \frac{P}{6bt} = 3.62 E_T \left(\frac{t}{b}\right)^2 \quad (1.28)$$

Equation (1.28) provides the optimum dimensions  $d$  and  $t$  as

$$t_{\text{opt}} = 0.289 \left(\frac{P^2 L}{E_T^2}\right)^{1/5} \quad (1.29a)$$

$$b_{\text{opt}} = 0.519 \left(\frac{P L^3}{E_T}\right)^{1/5} \quad (1.29b)$$

Substituting  $d_{\text{opt}}$  and  $t_{\text{opt}}$  from equations (1.29a,b) into any one of the three parts of equation (1.28) gives the optimum stress. Dividing by  $\rho$  gives the objective function:

$$\left(\frac{\sigma}{\rho}\right)_{\text{opt}} = 1.112 \left(\frac{E_T^{3/5}}{\rho}\right) \left(\frac{P}{L^2}\right)^{2/5} \quad (1.30)$$

*Method 2*

A check on equation (1.30) is provided by an alternative non-dimensional analysis in which the optimum stress is taken as the product of fractional powers in  $\sigma_F$ ,  $\sigma_W$  and  $\sigma_L$ . We may write this from equations (1.25)–(1.27) in two ways:

$$\sigma_{\text{opt}} = \sigma_F^\alpha \sigma_W^\beta \sigma_L^\gamma = \left( \frac{5\pi^2 E b^2}{12L^2} \right)^\alpha \left( \frac{P}{6bt} \right)^\beta \left[ 3.62 E_T \left( \frac{t}{b} \right)^2 \right]^\gamma$$

from which equalities between the indices in stress and the dimensions  $b$  and  $t$  follow:

$$[\sigma] : \alpha + \beta + \gamma = 1$$

$$[t] : -\beta + 2\gamma = 0$$

$$[b] : 2\alpha - \beta - 2\gamma = 0$$

giving:  $\alpha = 2/5$ ,  $\beta = 2/5$  and  $\gamma = 1/5$ . Consequently,

$$\begin{aligned} \sigma_{\text{opt}} &= \left( \frac{5\pi^2 E_T b^2}{12L^2} \right)^{2/5} \left( \frac{P}{6bt} \right)^{2/5} \left[ 3.62 E_T \left( \frac{t}{b} \right)^2 \right]^{1/5} \\ &= \left( \frac{5\sqrt{3.62}\pi^2}{12 \times 6} \right)^{2/5} E_T^{3/5} \left( \frac{P}{L^2} \right)^{2/5} \end{aligned}$$

in which the shape coefficient value of 1.112 in equation (1.30) is confirmed.

The exponents within the material efficiency factor  $M$  and the structural index  $S$  differ from those for the circular tube but are identical to those found for the square tube. In fact, all regular polygons conform to a similar, optimum objective function expression. This fact is a consequence of the stress in any closed, regular polygon arising from similar causes: flexure and local buckling of the plate within each side wall. This function appears consistently as

$$R = \left( \frac{\sigma}{\rho} \right)_{\text{opt}} = F \times M \times S^n \quad (1.31)$$

where  $n = 2/5$ ,  $M = E_T^{3/5}/\rho$ ,  $S = P/L^2$  and  $F$  varies as in Table 1.3. The differences in their shape efficiency factors  $F$  are attributed in part to the different local buckling coefficients  $K_L$ , when the polygon has an odd number of sides (see Table 1.3). The explanation given for this is that while each side of an even-sided polygon is simply supported, an odd number of sides has a partial restraint that depends upon the wavelength of buckling [5]. Despite this,  $F$  is seen to increase with the number of sides, though this is limited when the sides of a multiple-sided polygon do not remain straight [6]. We will see, however, that closed tubes are always more efficient than thin-walled open sections. Attempts to improve the structural efficiency of a strut further using closed cellular sections have only been partially successful. The triangular and square tubes

with matching interior honeycomb show no improvement irrespective of the number of cells, i.e.  $F$  is unchanged as the gains in local buckling and flexural buckling stresses are cancelled by the weight increase. While interior hexagonal cells provide a marginal benefit, a better alternative appears to be where a cellular wall in each geometry retains its hollow interior. For example, when a square tube has 10 square cells within each of its 4 walls  $F$  is raised to 1.42, compared to 0.907 for an ‘uninterrupted’ wall in Table 1.3.

It is left as an exercise for the reader to confirm the shape factors given in Table 1.3 for regular polygons with seven sides and more.

## 1.5 Thin-Walled, Open Sections

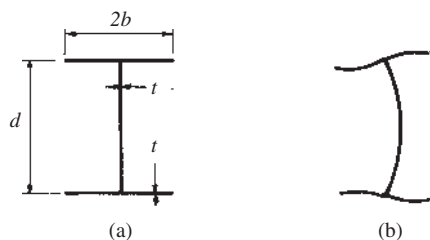
The objective function is again  $R = \sigma/\rho$  but more cross-sectional dimensions will require optimisation within the straight limbs of an open section. Moreover, given the particular shape (I, T, L, U, etc.), it is necessary to: (i) ensure that flexural buckling occurs about its two principal axes simultaneously and (ii) establish whether the flange or web is less resistant to local buckling. There follows the usual procedure of ensuring that critical stresses by the governing criteria are attained simultaneously. This condition will serve to optimise the section and thereafter allow the objective function  $R$  to be determined.

### 1.5.1 I-Section of Uniform Thickness

With  $2b$  and  $d$  as the section’s mean outer dimensions (Figure 1.8a), the modes of local buckling for a uniform I-section are shown in Figure 1.8b. For the optimum design condition both the flange and the web are taken as plates that buckle in flexure under a critical compressive stress. The web has both its long edges simply supported at the flange connection. Each flange half-length has one edge simply-supported and the other edge free.

#### (i) Flexural Buckling

Firstly, it is noted that  $k$  in equation (1.2b) is identified with the least second moment of area for the strut section. However, by allowing  $b$  and  $d$  to vary we can ensure that centroidal axes  $x$  and  $y$  are equally resistant to buckling, as was the case with our two earlier tube examples. Of course, in practice, flexural buckling would only occur about one axis only due to a slight eccentricity in the load axis and material imperfections. That  $k$  has equal values for the section about axes  $x$  and  $y$  in Figure 1.8a, follows from setting



**Figure 1.8** I-section showing local web and flange buckling

$I_x = I_y$ . This gives

$$2 \left[ 2bt \left( \frac{d}{2} \right)^2 \right] + \frac{t(d-t)^3}{12} = 2 \left[ \frac{t(2b)^3}{12} \right] + \frac{(d-t)t^3}{12} \quad (1.32a)$$

Provided  $t \ll d$  and  $t \ll b$  the final term on the right-hand side of equation (1.32a) may be ignored. This also allows us to set  $d-t \simeq d$  in the second term, leading to a cubic equation in  $b/d$ :

$$16(b/d)^3 - 12(b/d) - 1 = 0 \quad (1.32b)$$

Of the three roots of equation (1.32b),  $b/d = 0.905$ ,  $-0.821$  and  $-0.084$ , the one viable solution is  $b/d = 0.905$ , which corresponds to the  $I$  values

$$I_x = I_y = 2 \left[ \frac{(2 \times 0.905 d)^3 t}{12} \right] = 0.988 d^3 t \quad (1.33a)$$

The section area is

$$\begin{aligned} A &= 4bt + (d-t)t \approx 4bt + dt \\ &= 4(0.905 d)t + dt = 4.62 dt \end{aligned} \quad (1.33b)$$

when from equations (1.33a,b):

$$k^2 = \frac{I_x}{A} = \frac{0.988 d^3 t}{4.62 dt} = 0.214 d^2 \quad (1.33c)$$

Hence, from equations (1.33c) and (1.2b) the buckling stress becomes

$$\sigma_F = \frac{\pi^2 E_T (0.214 d^2)}{L^2} = \frac{2.112 E_T d^2}{L^2} \quad (1.34)$$

### (ii) Limiting Stress

The working, compressive stress in this strut becomes

$$\sigma_W = \frac{P}{A} = \frac{P}{4bt + dt} = \frac{P}{4.62 dt} \quad (1.35)$$

where  $\sigma_W \leq \sigma_y$ , for a proof stress  $\sigma_y$  defined by an offset strain (typically 0.1% or 0.2%). The gradient to the stress–strain curve, corresponding to  $\sigma_y$ , defines the tangent modulus  $E_T$  in equation (1.34).

### (iii) Local Buckling

Referring to Figure 1.8b, when the ends of the web are assumed to be simply supported, the stress condition required for it to bow, as shown in Figure 1.8b, is given by equation (1.20),

$$\sigma_L = 3.62 E_T \left( \frac{t}{d} \right)^2 \quad (1.36a)$$

for  $\nu = 0.3$ . Equation (1.20) will also apply to the stress for local flange buckling, when it is written as [3]:

$$\sigma_L = K_L E_T \left( \frac{t}{b} \right)^2 \quad (1.36b)$$

where, because one end is free,  $K_L$  is lowered to 0.385 [7]. Moreover, with a flange/web ratio  $b/d = 0.905$  we have, from equation (1.36b), the stress condition for local buckling in each of the four half-flanges:

$$\sigma_L = 0.385 E_T \left( \frac{t}{0.905 d} \right)^2 = 0.470 E_T \left( \frac{t}{d} \right)^2 \quad (1.36c)$$

Comparing equations (1.36a) and (1.36c) shows that flange will buckle well before the web. Hence, equation (1.36c) provides the local buckling criterion for an I-section with uniform thickness.

*(iv) Optimisation*

An optimum geometry is found by combining the criteria (i), (ii) and (iii) above to make the stresses by equations (1.34), (1.35) and (1.36c) equal,  $\sigma_F = \sigma_W = \sigma_L$ , which gives

$$\frac{2.112 E_T d^2}{L^2} = \frac{P}{4.62dt} = 0.470 E_T \left( \frac{t}{d} \right)^2 \quad (1.37)$$

Taking the components of equation (1.37) in pairs allows optimum dimensions  $d$  and  $t$  to be found:

$$t_{\text{opt}} = 0.630 \left( \frac{P^2 L}{E_T^2} \right)^{1/5}, \quad d_{\text{opt}} = 0.546 \left( \frac{P L^3}{E_T} \right)^{1/5} \quad (1.38a,b)$$

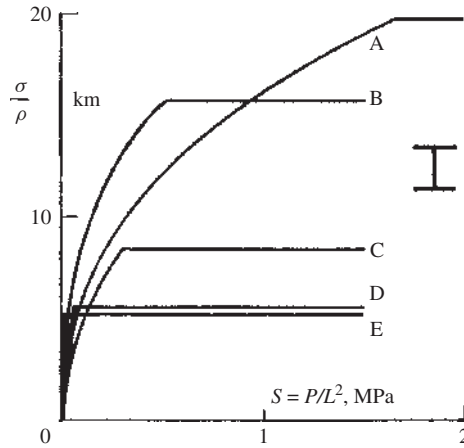
The optimum stress follows from substituting  $d_{\text{opt}}$  and  $t_{\text{opt}}$  from equation (1.38a,b) into any one of the three (now equal) stress expressions  $\sigma_F$ ,  $\sigma_W$ , or  $\sigma_L$  respectively in equation (1.37). Then, dividing by  $\rho$  gives the optimum, equivalent objective function:

$$\left( \frac{\sigma}{\rho} \right)_{\text{opt}} = 0.629 \left( \frac{E_T^{3/5}}{\rho} \right) \left( \frac{P}{L^2} \right)^{2/5} \quad (1.39)$$

Figure 1.9 presents equation (1.39) graphically for four materials whose properties and relevant ratios appear in Table 1.1.

Here the structural index  $S$  is reduced twofold compared to closed, thin-walled tubes. Within this restricted range, aluminium alloy (L65) is the most efficient material in raising the objective function to 15 km when  $S \approx 0.5$ , but titanium alloy extends  $S$  to beyond 1.5, raising the objective function to  $\approx 20$  km. Figure 1.10 compares four sections in the titanium alloy, including a solid square, two closed tubes and an I-section.

This shows that both the shape and material efficiency factors influence these plots, along with the appropriate exponent on the structural index  $S$ . Clearly, for a given  $S < 0.5$ ,



**Figure 1.9** Objective function versus  $S$  for I-section struts with uniform thickness (key: A, Ti alloy; B, Al alloy; C, steel; D, GFRC; E, Douglas fir (see Table 1.1))

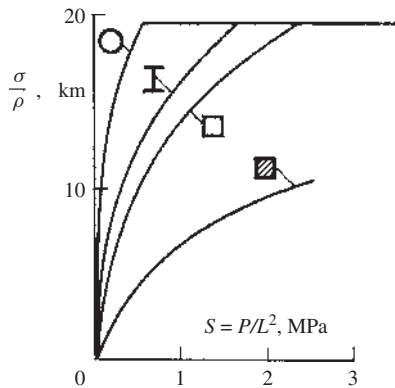
the circular tube is most efficient in supporting a compressive load. Note that an extended range for  $S$  appears in the earlier figures. For example, Figure 1.3 shows a maximum value of  $S \approx 10$  at the stress limit for a solid square section in titanium.

*1.5.2 Non-Uniform I-Section*

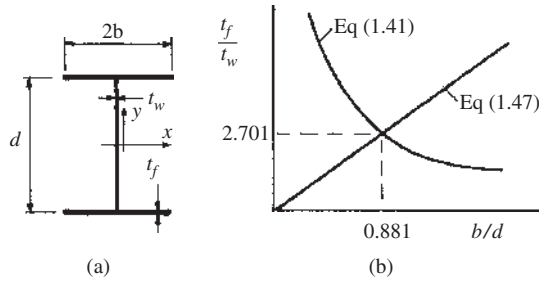
The dimensions of an I-section having different web and flange thicknesses are shown in Figure 1.11a.

*(i) Flexural Buckling*

With  $2b$  and  $d$  as the section's mean outer dimensions and web and flange thicknesses  $t_w$  and  $t_f$  respectively, the axes  $x$  and  $y$  are made equally least resistant to buckling when



**Figure 1.10** Objective function versus  $S$  for Ti alloy struts in various cross-sections



**Figure 1.11** I-section showing web and flange geometry

$I_x = I_y$ . This gives

$$2 \left[ 2bt_f \left( \frac{d}{2} \right)^2 \right] + \frac{t_w(d-t_f)^3}{12} = 2 \left[ \frac{t_f(2b)^3}{12} \right] + \frac{(d-t_f)t_w^3}{12} \quad (1.40a)$$

Provided  $b$  and  $d$  are each more than an order of magnitude greater than  $t_f$  and  $t_w$ , a good approximation to equation (1.40a) is

$$2 \left[ 2bt_f \left( \frac{d}{2} \right)^2 \right] + \frac{t_w d^3}{12} = 2 \left[ \frac{t_f(2b)^3}{12} \right] \quad (1.40b)$$

Equation (1.40b) gives the required thickness ratio

$$\frac{t_f}{t_w} = \left[ 16 \left( \frac{b}{d} \right)^3 - 12 \frac{b}{d} \right]^{-1} \quad (1.41)$$

The right-hand side of equation (1.40b) gives

$$I_x = I_y = \frac{4}{3} b^3 t_f \quad (1.42a)$$

and the section area is

$$A = 4bt_f + (d-t_f)t_w \approx 4bt_f + dt_w \quad (1.42b)$$

Hence, from equations (1.42a,b),

$$k^2 = \frac{I_x}{A} = \frac{4b^3 t_f}{3(4bt_f + dt_w)} \quad (1.43c)$$

Substituting equation (1.43c) into equation (1.2b), the buckling stress becomes

$$\sigma_F = \frac{\pi^2 E_T}{L^2} \left[ \frac{4b^3 t_f}{3(4bt_f + dt_w)} \right] = \frac{4 E_T}{3} \left( \frac{\pi d}{L} \right)^2 \left[ \frac{(t_f/t_w)(b/d)^3}{1 + 4(t_f/t_w)b/d} \right] \quad (1.44)$$

*(ii) Limiting Stress*

The working, compressive stress within the strut is to be

$$\sigma_W = \frac{P}{A} = \frac{P}{4bt_f + dt_w} = \frac{P}{dt_w[1 + 4(t_f/t_w)b/d]} \quad (1.45)$$

where  $\sigma_W \leq \sigma_y$ , for a proof stress  $\sigma_y$  defined by an offset strain (typically 0.1% or 0.2%). Again, the gradient to the stress–strain curve at the stress level  $\sigma_y$  defines the tangent modulus  $E_T$  in equation (1.44).

*(iii) Local Buckling*

Local buckling expressions are similar to those discussed previously for a uniform I-section [6]. Allowing for the different thicknesses, local web buckling occurs under a critical stress:

$$\sigma_L = 3.62 E_T \left( \frac{t_w}{d} \right)^2 \quad (1.46a)$$

and local flange buckling occurs under the stress:

$$\sigma_L = 0.385 E_T \left( \frac{t_f}{b} \right)^2 \quad (1.46b)$$

Here we can arrange for web and flange buckling to occur simultaneously by equating the stresses in equations (1.46a,b). This gives

$$\frac{t_f}{t_w} = 3.066 \frac{b}{d} \quad (1.47)$$

*(iv) Optimisation*

Firstly, we equate the thickness ratio  $t_f/t_w$  from each of equations (1.41) and (1.47):

$$3.066 \frac{b}{d} \left[ 16 \left( \frac{b}{d} \right)^3 - 12 \frac{b}{d} \right] = 1 \quad (1.48)$$

Equation (1.48) may be reduced to a quadratic equation whose positive root leads to optimised geometric ratios:

$$\left( \frac{b}{d} \right)_{\text{opt}} = 0.881, \quad \left( \frac{t_f}{t_w} \right)_{\text{opt}} = 2.701 \quad (1.49a,b)$$

Alternatively, the graphical solution to equating (1.41) and (1.47) is shown in Figure 1.11b. Now, we equate  $\sigma_F$  to  $\sigma_W$ , from equations (1.44) and (1.45), to give

$$\frac{4 E_T}{3} \left( \frac{\pi d}{L} \right)^2 \left[ \frac{(t_f/t_w)(b/d)^3}{1 + 4(t_f/t_w)b/d} \right] = \frac{P}{dt_w[1 + 4(t_f/t_w)b/d]}$$

where, from equations (1.49a,b), we find

$$d^3 t_w = \frac{0.0411 P L^2}{E_T}$$

which leads to the optimum outer dimensions and thicknesses:

$$b_{\text{opt}} = 0.486 \left( \frac{P L^3}{E_T} \right)^{1/5}, \quad d_{\text{opt}} = 0.552 \left( \frac{P L^3}{E_T} \right)^{1/5} \quad (1.50\text{a,b})$$

$$t_{w\text{opt}} = 0.244 \left( \frac{P^2 L}{E_T^2} \right)^{1/5}, \quad t_{f\text{opt}} = 0.659 \left( \frac{P^2 L}{E_T^2} \right)^{1/5} \quad (1.51\text{a,b})$$

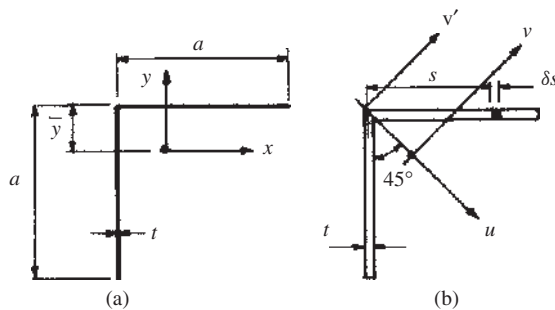
The optimum stress follows from substituting the appropriate optimum dimensions into any one of the three (now equal) stress expressions  $\sigma_F$ ,  $\sigma_W$ , or  $\sigma_L$  in equations (1.44)–(1.46). Dividing by  $\rho$  gives the optimum objective function

$$\left( \frac{\sigma}{\rho} \right)_{\text{opt}} = 0.705 \left( \frac{E_T^{3/5}}{\rho} \right) \left( \frac{P}{L^2} \right)^{2/5} \quad (1.52)$$

Equation (1.52) is similar in form to equation (1.39). Between equations (1.50)–(1.52) it can be seen how this optimised design increases the structural efficiency compared to an I-section with uniform thickness, where  $F = 0.629$ .

### 1.5.3 Equal-Angle

Though the equal-angle is the simplest thin-walled, open strut section (see Figure 1.12a), it is complicated by having principal axes of flexure at  $45^\circ$  to its long sides. As there is no web, a single local flange buckling criterion need only be combined with the criterion for flexural buckling about the principal axis with the lesser  $I$ -value.



**Figure 1.12** Equal-angle showing principal axes  $u$  and  $v$

*(i) Flexural Buckling*

Taking  $a$  as the mean side length, it is required to identify  $k$  in equation (1.2b) with the least second moment of area. With the side lengths being equal, it is not possible for the section to be equally resistant to buckling about its principal axes  $u$  and  $v$  in Figure 1.12b. That is,  $I_u \neq I_v$  and the lesser  $I$ -value follows, firstly, from locating the centroid position  $\bar{y} = (\bar{x})$  in Figure 1.12a:

$$(at)t/2 + at(a/2) = 2at\bar{y}, \quad \Rightarrow \quad \bar{y} = (a+t)/4 \simeq a/4 \quad (1.53)$$

With each limb being equally inclined to the  $u$ -axis (see Figure 1.12b),  $I_u = \int_A v^2 dA$  is applied with  $v = s \sin 45^\circ$  and  $dA = t ds$ . This gives:

$$I_u = 2 \int_0^a (s \sin 45^\circ)^2 \times t ds = \frac{a^3 t}{3} \quad (1.54a)$$

To find  $I_v$  we first find the second moment of the area about an axis  $v'$  passing through the corner (see Figure 1.11b) and then transfer it to the parallel centroidal axis  $v$  by using equation (1.53) and the parallel axis theorem:

$$\begin{aligned} I_v &= I_{v'} - Ah^2 = 2 \int_0^a (s \cos 45^\circ)^2 t ds - 2at(\sqrt{2}\bar{y})^2 \\ &= \frac{a^3 t}{3} - \frac{a^3 t}{4} = \frac{a^3 t}{12} \end{aligned} \quad (1.54b)$$

Clearly, from equations (1.54a,b),  $I_v$  is the lesser of the two  $I$ -values, from which

$$k^2 = \frac{I_v}{A} = \frac{a^3 t/12}{2at} = \frac{a^2}{24} \quad (1.55a)$$

Substituting equation (1.55a) into the buckling stress equation (1.2b) gives

$$\sigma_F = \frac{\pi^2 E_T a^2}{24L^2} \quad (1.55b)$$

*(ii) Limiting Stress*

The working, compressive stress for this strut is simply

$$\sigma_W = \frac{P}{A} = \frac{P}{2at} \quad (1.56)$$

where  $\sigma_W \leq \sigma_y$ , for a proof stress  $\sigma_y$  defined by an offset strain (typically 0.1% or 0.2%). The gradient to the stress–strain curve corresponding to  $\sigma_y$  defines the tangent modulus  $E_T$  in equation (1.55b). If  $\sigma_y$  lies at the limit of proportionality, then  $E$  replaces  $E_T$ .

(iii) *Local Buckling*

Referring to Figure 1.12a, a local buckling of both limbs occurs simultaneously when the stress attains its limiting value:

$$\sigma_L = K_L E_T \left( \frac{t}{a} \right)^2 \quad (1.57)$$

where, as for the previous section considered,  $K_L = 0.385$  for  $\nu = 0.3$  [3].

(iv) *Optimisation*

An optimum geometry is found by combining criteria (i), (ii) and (iii) above so that the stresses by equations (1.55)–(1.57) are made equal,  $\sigma_F = \sigma_W = \sigma_L$ , which gives

$$\frac{\pi E_T a^2}{24L^2} = \frac{P}{2at} = 0.385 E_T \left( \frac{t}{a} \right)^2 \quad (1.58)$$

Equation (1.58) allows optimum dimensions  $a$  and  $t$  to be found:

$$t_{\text{opt}} = 1.103 \left( \frac{P^2 L}{E_T^2} \right)^{1/5}, \quad a_{\text{opt}} = 1.033 \left( \frac{P L^3}{E_T} \right)^{1/5} \quad (1.59\text{a,b})$$

The optimum stress follows from substituting  $a_{\text{opt}}$  and  $t_{\text{opt}}$  into any one of the three (now equal) stress expressions  $\sigma_F$ ,  $\sigma_W$ , or  $\sigma_L$  in equation (1.58). Dividing by  $\rho$  gives this section's optimum objective function

$$\left( \frac{\sigma}{\rho} \right)_{\text{opt}} = 0.439 \left( \frac{E_T^{3/5}}{\rho} \right) \left( \frac{P}{L^2} \right)^{2/5} \quad (1.60)$$

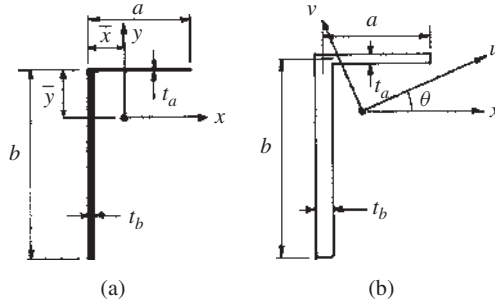
### 1.5.4 Unequal-Angle

The previous analysis of an equal-angle section suggests that a greater degree of optimisation is possible when the lengths  $a, b$  and thicknesses  $t_a, t_b$  of the two limbs are different. The principal axes of flexure will no longer lie at  $45^\circ$ . Again, the axis having the minimum second moment of area will control flexural buckling while, simultaneously, a local buckling in each limb can be arranged to occur for the optimum design. Here, we shall firstly equalise the local flange buckling stress for each limb. The constraint that this imposes upon the angle's geometry is then applied to the flexural buckling of an angle section with any limb length ratio  $L = b/a$ , where  $b > a$ , in Figure 1.13a.

(i) *Local Buckling*

If the limb lengths  $a$  and  $b$  and their respective thicknesses  $t_a$  and  $t_b$  are different, we can ensure that their local buckling occurs simultaneously. From equation (1.57), this condition gives

$$\sigma_L = K_L E_T \left( \frac{t_a}{a} \right)^2 = K_L E_T \left( \frac{t_b}{b} \right)^2 \quad (1.61\text{a})$$



**Figure 1.13** Unequal angle showing principal axes

where  $K_L = 0.385$ . Hence, the simple geometrical relationship

$$r = b/a = t_b/t_a \quad (1.61b)$$

follows from equation (1.61a).

(ii) *Flexural Buckling*

The centroidal coordinates,  $(\bar{x}, \bar{y})$  in Figure 1.13a, are found from

$$\begin{aligned} bt_b^2/2 + a^2t_a/2 = (at_a + bt_b)\bar{x}, & \Rightarrow \bar{x} \approx \frac{a}{2[1 + (b/a)(t_b/t_a)]} = \frac{a}{2(1 + r^2)} \\ at_a^2/2 + b^2t_b/2 = (at_a + bt_b)\bar{y}, & \Rightarrow \bar{y} \approx \frac{b}{2[1 + (a/b)(t_a/t_b)]} = \frac{br^2}{2(1 + r^2)} \end{aligned} \quad (1.62a,b)$$

The second moments of area, referred to centroidal axes  $x$  and  $y$ , are

$$\begin{aligned} I_x &= at_a\bar{y}^2 + t_b b^3/12 + bt_b(b/2 - \bar{y})^2 = \frac{a^3 t_a r^4 (r^2 + 4)}{12(1 + r^2)} \\ I_y &= bt_b\bar{x}^2 + t_a a^3/12 + at_a(a/2 - \bar{x})^2 = \frac{a^3 t_a (4r^2 + 1)}{12(1 + r^2)} \\ I_{xy} &= at_a(a/2 - \bar{x})\bar{y} + bt_b(b/2 - \bar{y})\bar{x} = \frac{a^3 t_a r^3}{4(1 + r^2)} \end{aligned} \quad (1.63a,b,c)$$

The principal second moments of area  $I_{u,v}$  and their orientation  $\theta$  with respect to axis  $x$  (see Figure 1.13b) are found from

$$\begin{aligned} I_u, I_v &= \frac{1}{2}(I_x + I_y) \pm \frac{1}{2}\sqrt{(I_x - I_y)^2 + 4I_{xy}^2} \\ \tan 2\theta &= 2I_{xy}/(I_x - I_y) \end{aligned} \quad (1.64a,b,c)$$

where  $I_u > I_v$  when  $\theta$  refers to the inclination of  $u$  with respect to  $x$  (see Figure 1.13b). Substituting equations (1.63a–c) into equation (1.64b), the lesser  $I$  is seen to be

$$I_v = \left[ \frac{(r^6 + 4r^4 + 4r^2 + 1) - \sqrt{(r^6 + 4r^4 - 4r^2 - 1)^2 + 36r^6}}{24(1 + r^2)} \right] a^3 t_a = \frac{a^3 t_a n(r)}{24(1 + r^2)} \quad (1.65a)$$

where the function  $n(r)$  is the expression in square brackets. The section area is

$$A = at_a + bt_b = at_a(1 + r^2) \quad (1.65b)$$

Dividing equations (1.65a,b), the least radius of gyration  $k^2 = I_v/A$  is written as

$$k^2 = \frac{a^2 n(r)}{24(1 + r^2)^2} \quad (1.65c)$$

It follows from equation (1.65c) that the buckling stress in equation (1.2b) becomes

$$\sigma_F = \frac{\pi^2 E_T a^2 n(r)}{24(1 + r^2)^2 L^2} \quad (1.66)$$

(iii) *Limiting Stress*

The working, compressive stress in the strut is given as

$$\sigma_W = \frac{P}{A} = \frac{P}{at_a + bt_b} = \frac{P}{at_a(1 + r^2)} \quad (1.67)$$

where  $\sigma_W \leq \sigma_y$ , for a proof stress  $\sigma_y$  defined by an offset strain (typically 0.1% or 0.2%). The gradient to the stress–strain curve, corresponding to  $\sigma_y$ , defines the tangent modulus  $E_T$  in equation (1.66).

(iv) *Optimisation*

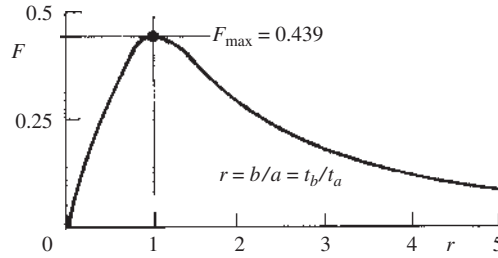
An optimum geometry is found by combining criteria (i), (ii) and (iii) above so that the stresses by equations (1.61), (1.66) and (1.67) are made equal,  $\sigma_F = \sigma_W = \sigma_L$ , which gives

$$\frac{\pi^2 E_T a^2 n(r)}{24(1 + r^2)^2 L^2} = \frac{P}{at_a(1 + r^2)} = 0.385 E_T \left( \frac{t_a}{a} \right)^2 \quad (1.68)$$

Equation (1.68) allows the optimum dimensions  $a_{\text{opt}}$  and  $(t_a)_{\text{opt}}$  to be found for an angle-section with a particular  $R = b/a$  value:

$$(t_a)_{\text{opt}} = \frac{1.455}{\{(1 + r^2)^2 [n(r)]\}^{1/10}} \left( \frac{P^2 L}{E_T^2} \right)^{1/5} \quad (1.69a,b)$$

$$a_{\text{opt}} = 1.187 \left\{ \frac{(1 + r^2)^4}{[n(r)]^3} \right\}^{1/10} \left( \frac{P L^3}{E_T} \right)^{1/5}$$



**Figure 1.14** Dependence of shape function  $F$  upon limb ratio  $r$

Correspondingly, the optimum stress follows from substituting  $a_{\text{opt}}$  and  $(t_a)_{\text{opt}}$  into any one of the three (now equal) stress expressions  $\sigma_F$ ,  $\sigma_W$ , or  $\sigma_L$  in equation (1.68). Dividing by  $\rho$  gives the objective function:

$$\left(\frac{\sigma}{\rho}\right)_{\text{opt}} = 0.579 \left[ \frac{n(r)}{(1+r^2)^3} \right]^{2/5} \left( \frac{E_T^{3/5}}{\rho} \right) \left( \frac{P}{L^2} \right)^{2/5} = f \left( \frac{E_T^{3/5}}{\rho} \right) \left( \frac{P}{L^2} \right)^{2/5} \quad (1.70)$$











Now it becomes clear that if the strut weight is to be minimised, how this optimum stress should be maximised. Thus, for a strut of given material, length and loading, a maximum for the coefficient term in  $r$  is required. Identifying this coefficient term within the shape efficiency factor,  $F = 0.579[n(r)/(1+r^2)^3]^{2/5}$ , the value of  $r$  that maximises  $F$  is shown in Figure 1.14.

Having used  $r = b/a = t_b/t_a$  for the above analysis, the graph shows that it is the equal angle, i.e.  $r = 1$ , which has the minimum weight possible for this condition. Hence the shape efficiency factor expression in equation (1.70) reduces to  $F = 0.439$ , agreeing with that found previously for an equal-angle. The optimum values of  $F$ , for  $1 < r \leq 5$  may be read from the graph. It is left as an exercise for the reader to investigate the effect upon the optimum condition of any alternative geometric constraint to that in equation (1.61b). For example, BS sections [8] use  $R = 1.16, 1.2, 1.33, 1.5, 1.6, 2, 2.25$ , with thicknesses having an inner taper.

## 1.6 Summary of Results

Table 1.4 summarises the results for the objective functions of the 11 strut sections considered here. It is seen that only the structural index  $S = P/L^2$  is common to all sections. However, its exponent  $n$  differs along with the material efficiency factor within the three categories of section shown in Table 1.4. These categories refer to flexural buckling only and flexural buckling combined with local buckling in curved and flat plates. Where more than one section lies within a given category it becomes possible to compare their shape efficiency factors. Given the inverse relationship between the equivalent objective function and the weight, we may conclude that those strut sections which minimise weight in solid, closed and open sections most effectively are: (i) a solid

**Table 1.4** Equivalent objective functions for various struts:  
 $R = F \times M \times S^n$  [ $R = (\sigma/\rho)_{opt}$ ,  $S = P/L^2$ ]

Cross-section	Shape efficiency factor $F$	Material efficiency factor $M$	Exponent $n$
	0.886	$E_T^{1/2}/\rho$	1/2
	0.907	$E_T^{1/2}/\rho$	1/2
	0.663	$E_T^{1/2}/\rho$	1/2
	0.975	$E_T^{1/2}/\rho$	1/2
	0.540	$E_T^{2/3}/\rho$	1/3
	0.907	$E_T^{3/5}/\rho$	2/5
	1.112	$E_T^{3/5}/\rho$	2/5
	0.630	$E_T^{3/5}/\rho$	2/5
	0.705	$E_T^{3/5}/\rho$	2/5
	0.439	$E_T^{3/5}/\rho$	2/5

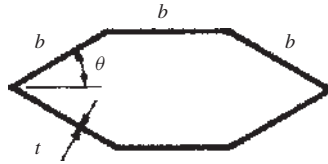
square, (ii) a regular, thin-walled, hexagonal tube and (iii) a non-uniform I-section.

**References**

[1] Timoshenko, S. J. and Gere, J. M. *Theory of Elastic Stability*, McGraw-Hill, 1961.  
 [2] ESDU 78021, Guide to items on the strength and stability of struts, October 1978.  
 [3] ESDU 72019, Buckling of flat isotropic plates under uniaxial and biaxial loading, August 1972.  
 [4] Gerard, G. Compressive and torsional buckling of thin-walled cylinders in the yield region, NACA Tech. Note 3726, August 1956.  
 [5] Cox, H. L. *The Design of Structures of Least Weight*, Pergamon, 1965.  
 [6] ESDU 01.01.08, Local instability of struts with flat sides, November 1990.  
 [7] ESDU 78020, Local buckling and crippling of I, Z and channel section struts, July 1978.  
 [8] BS 4848 Part 2: 1991, Specifications for hot rolled structural steel sections: unequal angles.

**Exercises**

**1.1** Confirm the shape factors  $C$  and  $F$ , given in Table 1.2, that appear within the optimum dimension and the objective function for pinned-end struts, having the following cross-sections: (i) a solid semi-circle, diameter  $d$ , and (ii) an equilateral triangle, side length  $a$ .



**Figure 1.15** Flattened hexagonal tube

**1.2** Using the local buckling coefficients  $K_L$ , listed in Table 1.3, confirm those shape efficiency factors  $F$  given for regular polygons with seven sides and more.

**1.3** When the regular hexagonal tube in Section 1.4.3 is flattened so that the included angle  $\theta$  is not  $60^\circ$ , the second moments of area about the  $x$ - and  $y$ -axes are no longer equal. Examine the effect upon the shape efficiency factor  $F$  when: (i)  $0^\circ < \theta < 45^\circ$  and (ii)  $45^\circ < \theta < 90^\circ$  (see Figure 1.15). Confirm the known result in Table 1.3 for when  $\theta = 60^\circ$  in each case. [Answer: (i)  $F = 1.248(\sin \theta)^{4/5}$ ]

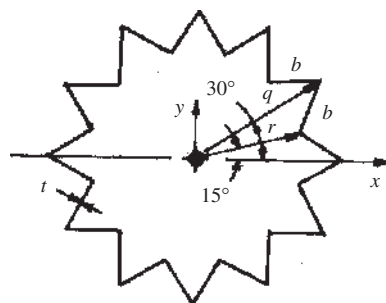
**1.4** A long, aluminium-alloy strut ( $E = 70$  GPa), with a uniformly square, tubular cross-section and pinned ends, is required to bear a compressive load of 10 kN in a 2 m length. Obtain the values of the mean side length  $a$  and wall thickness  $t$  that will minimise the weight (i.e. minimise the section area). Show this graphically in a plot of the objective function against cross-section areas ranging from  $100 \text{ mm}^2$  to  $350 \text{ mm}^2$  in steps of  $50 \text{ mm}^2$ . Construct a 2D design space with boundaries fixed by the following constraints:

- (i) flexural buckling must not occur;
- (ii) local buckling of the walls is to be avoided;
- (iii)  $a$  must lie in the range  $40 \leq a \leq 100$  mm;
- (iv)  $t$  must lie in the range  $0.9 \leq t \leq 2.5$  mm.

**1.5** Investigate the optimum design condition for a strut with an unequal angle section where  $t_b/b < t_a/a$ , such that local buckling occurs only in the longer limb.

**1.6** Investigate the optimum design condition for a strut having an unequal angle section with  $b/a = 3$  and constant thickness such that local buckling occurs only in the longer limb.

**1.7** A long, thin-walled, regular hexagonal tube in steel is to support a compressive load of 20 kN over its 5 m pinned length. Construct a 2D design space bounded by the following requirements:



**Figure 1.16** Tubular strut having 12 vee-corrugations

- (i) flexural buckling must not occur
- (ii) local buckling of the four walls must not occur
- (iii) the mean side length is to lie between 150 mm and 200 mm
- (iv) the wall thickness is to lie between 2.5 mm and 5 mm.

Find the side wall dimensions  $a$  and  $t$  which minimise the area and so the weight. Take  $E = 210$  GPa.

**1.8** A strut is made in the form of a closed tube with 12 vee-corrugations, each having flats  $b \times t$ , as shown in Figure 1.16. Derive an expression for the second moment of area in terms of the geometry given about the axis  $x$ . Is this the least value for the section? Derive the objective function when flexural and local buckling occur together under a limiting compressive stress  $\sigma_y$ . Hence, find the shape efficiency factor and compare with that for a thin, circular tube.

